

# A Novel, Smart Microsphere with K<sup>+</sup>-Induced Shrinking and Aggregating Properties Based on a Responsive Host–Guest System

Ming-Yue Jiang,<sup>†</sup> Xiao-Jie Ju,<sup>\*,†</sup> Lu Fang,<sup>†</sup> Zhuang Liu,<sup>†</sup> Hai-Rong Yu,<sup>†</sup> Lu Jiang,<sup>§</sup> Wei Wang,<sup>†</sup> Rui Xie,<sup>†</sup> Qianming Chen,<sup>§</sup> and Liang-Yin Chu<sup>\*,†,‡</sup>

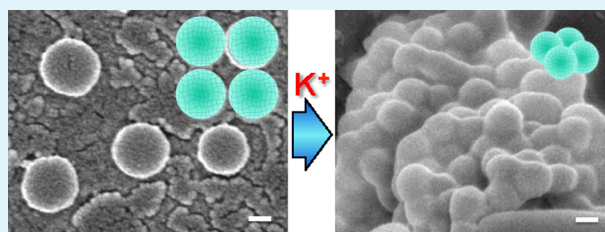
<sup>†</sup>School of Chemical Engineering, Sichuan University, Chengdu, Sichuan 610065, P. R. China

<sup>§</sup>State Key Laboratory of Oral Diseases, Sichuan University, Chengdu, Sichuan 610041, P. R. China

<sup>‡</sup>State Key Laboratory of Polymer Materials Engineering and Collaborative Innovation Center for Biomaterials Science and Technology, Sichuan University, Chengdu, Sichuan 610065, P. R. China

**ABSTRACT:** A novel type of smart microspheres with K<sup>+</sup>-induced shrinking and aggregating properties is designed and developed on the basis of a K<sup>+</sup>-recognition host–guest system. The microspheres are composed of cross-linked poly(*N*-isopropylacrylamide-*co*-acryloylamidobenzo-15-crown-5) (P-(NIPAM-*co*-AAB15C5)) networks. Due to the formation of stable 2:1 “sandwich-type” host–guest complexes between 15-crown-5 units and K<sup>+</sup> ions, the P(NIPAM-*co*-AAB15C5) microspheres significantly exhibit isothermally and synchronously K<sup>+</sup>-induced shrinking and aggregating properties at a low K<sup>+</sup> concentration, while other cations (e.g., Na<sup>+</sup>, H<sup>+</sup>, NH<sub>4</sub><sup>+</sup>, Mg<sup>2+</sup>, or Ca<sup>2+</sup>) cannot trigger such response behaviors. Effects of chemical compositions of microspheres on the K<sup>+</sup>-induced shrinking and aggregating behaviors are investigated systematically. The K<sup>+</sup>-induced aggregating sensitivity of the P(NIPAM-*co*-AAB15C5) microspheres can be enhanced by increasing the content of crown ether units in the polymeric networks; however, it is nearly not influenced by varying the monomer and cross-linker concentrations in the microsphere preparation. State diagrams of the dispersed-to-aggregated transformation of P(NIPAM-*co*-AAB15C5) microspheres in aqueous solutions as a function of temperature and K<sup>+</sup> concentration are constructed, which provide valuable information for tuning the dispersed/aggregated states of microspheres by varying environmental K<sup>+</sup> concentration and temperature. The microspheres with synchronously K<sup>+</sup>-induced shrinking and aggregating properties proposed in this study provide a brand-new model for designing novel targeted drug delivery systems.

**KEYWORDS:** microspheres, K<sup>+</sup>-recognition, responsive host–guest system, phase transition, aggregation



## INTRODUCTION

Potassium ion (K<sup>+</sup>) plays an important role in biological systems. K<sup>+</sup> not only is involved in the maintenance of extracellular/intracellular osmotic pressure, pH value, and normal metabolism but also regulates the concentration of other ions in the cell.<sup>1</sup> The normal concentration of serum K<sup>+</sup> in the human body is in the range of 3.5–5.5 mmol L<sup>-1</sup>. The value of the intracellular K<sup>+</sup> concentration is about 30 times of the extracellular K<sup>+</sup> concentration.<sup>2</sup> Certain diseases can cause a disorder of extracellular/intracellular K<sup>+</sup> concentration. For example, necrocytosis at specific pathological sites and a defect in the K<sup>+</sup>–Na<sup>+</sup> pump in the cell membrane would result in an abnormal increase of extracellular K<sup>+</sup> concentration.<sup>3</sup> Thus, the abnormal increase of K<sup>+</sup> concentration can be treated as a disease signal, and drug delivery systems that can recognize this stimulus signal for K<sup>+</sup>-triggered controlled-release will be of great significance. Functional microspheres are promising candidates as drug carriers and biosensors due to their micron size, large specific surface area, and functional properties.<sup>4–15</sup> Site-specific aggregation of microspheres at certain organs or tissues is beneficial to the site-targeting, which is crucial to

targeted drug delivery systems.<sup>16–18</sup> Therefore, smart microspheres with K<sup>+</sup>-induced aggregating properties as targeted drug delivery systems are of great importance.

Crown ethers are known for the unique property of formation of stable host–guest complexes with alkali metal ions. For example, 18-crown-6 can selectively recognize and capture K<sup>+</sup> by forming stable 1:1 “host–guest” 18-crown-6/K<sup>+</sup>.<sup>19</sup> It has been reported that cross-linked poly(*N*-isopropylacrylamide-*co*-benzo-18-crown-6-acrylamide) (P-(NIPAM-*co*-B18C6Am)) microspheres slightly exhibit a K<sup>+</sup>-induced swelling property but the swelling degree is not significant, and the microspheres show an aggregating property only in the case of high K<sup>+</sup> concentration (e.g., ≥15 mM).<sup>20</sup> However, in certain applications, such as K<sup>+</sup>-triggered release of drugs, an inverse mode of K<sup>+</sup>-responsive volume change behavior (i.e., K<sup>+</sup>-induced shrinking) of the microspheres is preferred. Besides, the K<sup>+</sup>-induced aggregating sensitivity to lower K<sup>+</sup>

**Received:** August 15, 2014

**Accepted:** October 17, 2014

**Published:** October 17, 2014

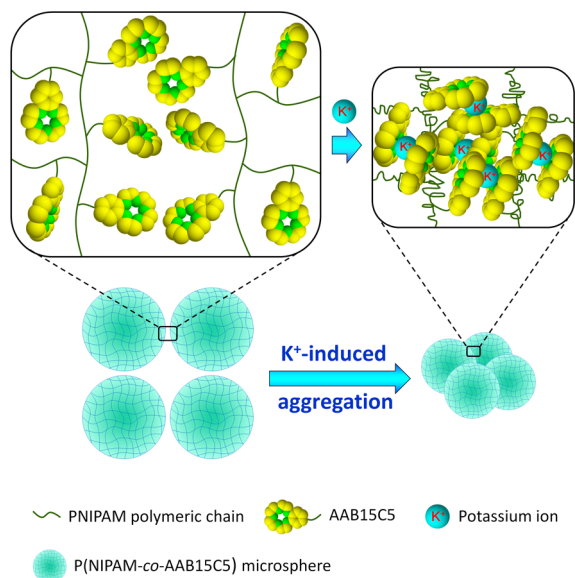


**Figure 1.** Schematic illustration of the  $K^+$ -induced shrinking and aggregating behavior of P(NIPAM-*co*-AAB15C5) microspheres upon formation of stable 2:1 “sandwich-type” complexes of pendent 15-crown-5 receptors and  $K^+$  ions.

concentration is very important in biomedical applications. Unfortunately, to the best of our knowledge, such a kind of smart microspheres with isothermally and synchronously  $K^+$ -induced shrinking and aggregating property has not been reported yet.

Here, we report on a novel type of smart microspheres with  $K^+$ -induced shrinking and aggregating properties based on a responsive host–guest system. The microspheres are composed of cross-linked poly(*N*-isopropylacrylamide-*co*-acryloylamido-benzo-15-crown-5) (P(NIPAM-*co*-AAB15C5)) networks, in which pendent 15-crown-5 units act as  $K^+$ -recognition receptors and poly(*N*-isopropylacrylamide) (PNIPAM) units act as actuators. When  $K^+$  appears in the environment, the adjacent 15-crown-5 receptors capture  $K^+$  to form stable 2:1 “sandwich-type” host–guest complexes within and among microspheres,<sup>21–25</sup> which would disrupt the hydrogen bonding between the oxygen atoms in 15-crown-5 and the hydrogen atoms of water and cause the copolymer chains to contract rapidly; as a result, microspheres significantly exhibit an isothermal shrinkage and aggregation phenomenon by recognizing  $K^+$  (Figure 1). The microspheres are prepared by a two-step reaction method combining precipitation copolymerization<sup>20</sup> and chemical modification,<sup>26</sup> so that enough 15-crown-5 units can be fixed onto the polymeric networks of the microspheres to ensure that the  $K^+$ -induced aggregation can be

**Table 1. Recipe for Preparation of P(NIPAM-*co*-AAc) Microspheres**

code	[NIPAM] + [AAc] (mol/L)	[AAc]/([NIPAM] + [AAc]) (mol %)	[MBA]/([NIPAM] + [AAc]) (mol %)
#1	0.1	20	2.6
#2	0.1	10	2.6
#3	0.1	30	2.6
#4	0.1	20	1.0
#5	0.1	20	5.0
#6	0.2	20	2.6
#7	0.3	20	2.6

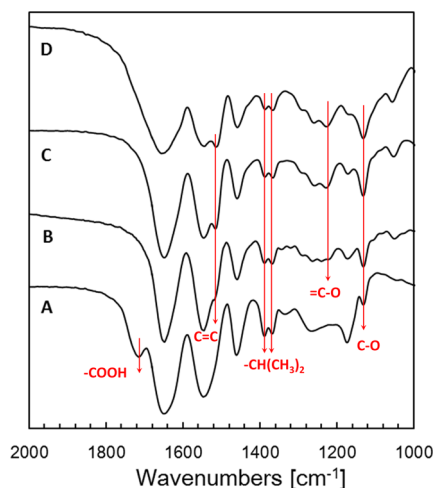


**Figure 2.** FT-IR spectra of P(NIPAM-*co*-AAc) microsphere prepared with 10% (Curve A) of AAc feed molar content and P(NIPAM-*co*-AAB15C5) microspheres prepared with 10% (Curve B), 20% (Curve C), and 30% (Curve D) of AAc feed molar contents.

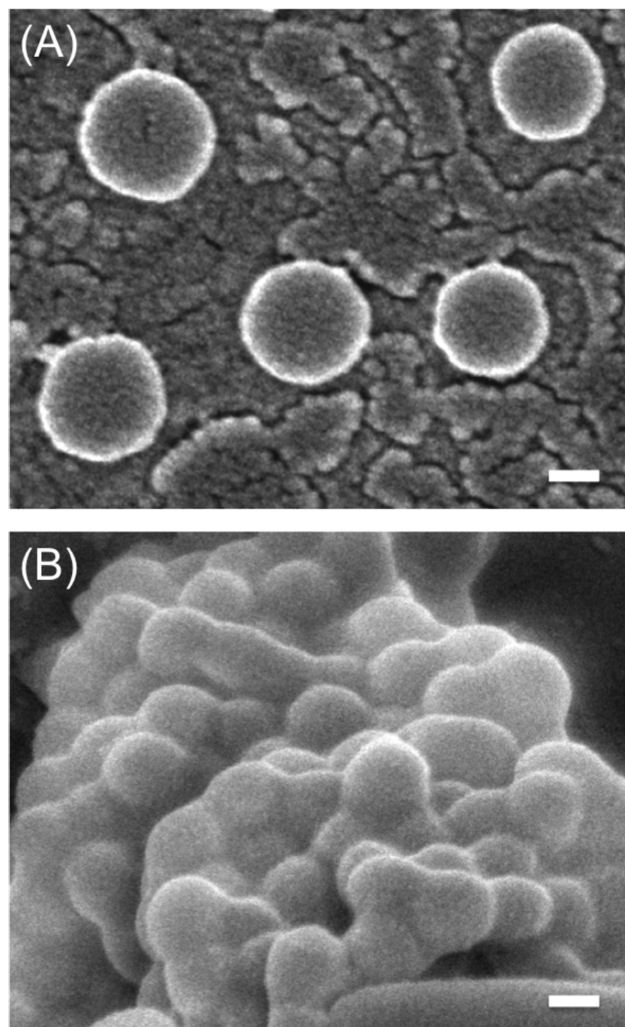


**Figure 3.** SEM images of dispersed P(NIPAM-*co*-AAB15C5) microspheres in the absence of  $K^+$  ions (A) and aggregated P(NIPAM-*co*-AAB15C5) microspheres in the presence of  $K^+$  ions (B). Scale bars are 100 nm.

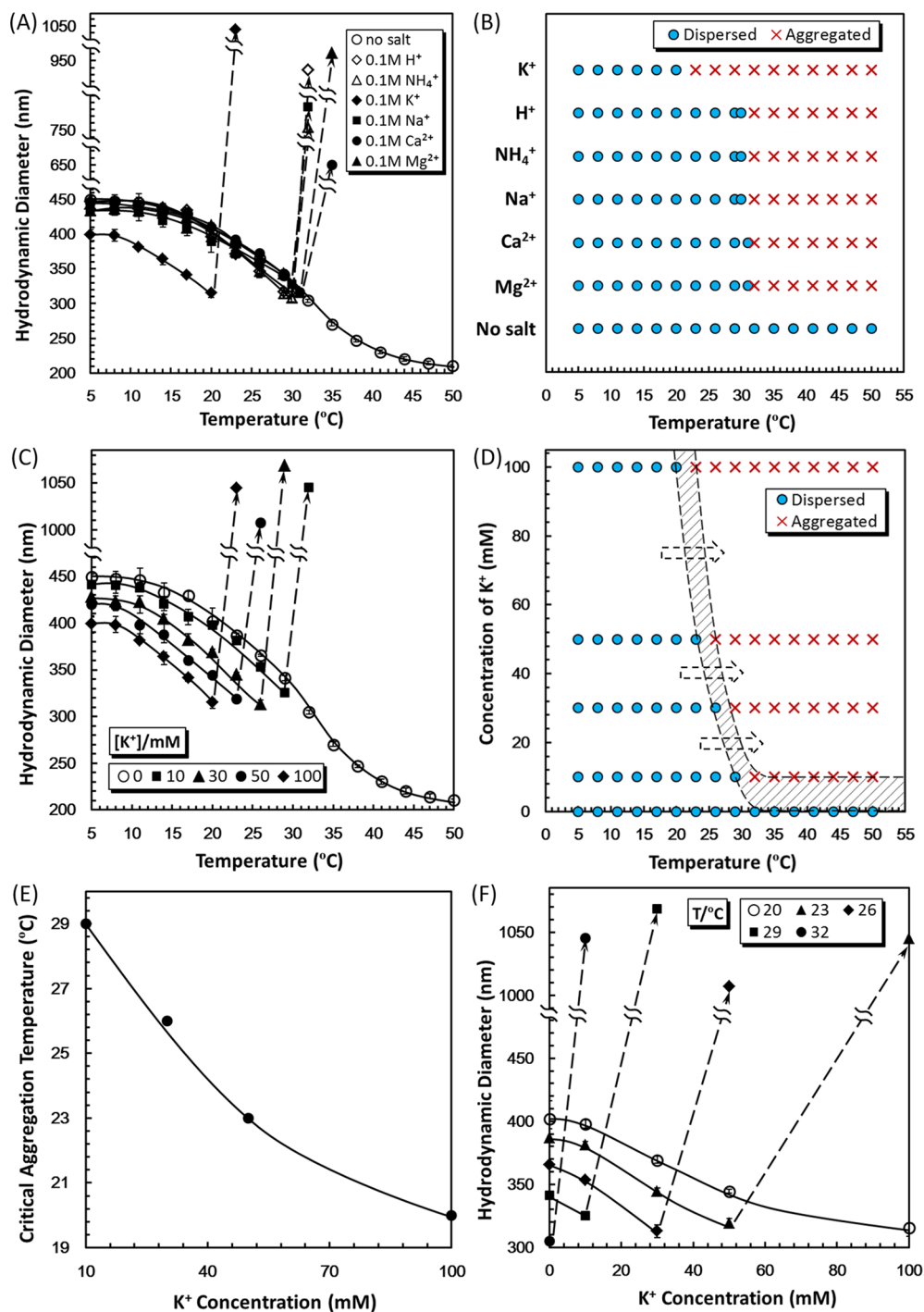


**Figure 4.** Effects of ion species (A, B) and  $K^+$  concentration (C, D, E, F) on the isothermal shrinking and aggregating behaviors of P(NIPAM-co-AAB15C5) microspheres. (A, C) Hydrodynamic diameters of microspheres in deionized water and various cation solutions as a function of temperature. (B, D) State diagram of the dispersed-to-aggregated transformation of microspheres in deionized water and various cation solutions as a function of temperature. (E) Relationship between the  $K^+$  concentration and the critical aggregation temperature. (F) Relationship between the  $K^+$  concentration and the hydrodynamic diameter of the microspheres under a certain temperature condition.

achieved effectively under the condition of low  $K^+$  concentration. Effects of chemical compositions of microspheres and the environmental  $K^+$  concentration and temperature on the  $K^+$ -induced shrinking and aggregating behaviors are investigated systematically. State diagrams of the dispersed-to-aggregated transformation of P(NIPAM-co-AAB15C5) microspheres as a function of temperature and  $K^+$  concentration are constructed according to the experimental data. The results in

this study provide valuable guidance for designing novel targeted drug delivery systems with  $K^+$ -induced shrinking and aggregating properties.

## MATERIALS AND METHODS

**Materials.** *N*-Isopropylacrylamide (NIPAM, purchased from Sigma-Aldrich) is purified by recrystallization with a hexane/acetone mixture (v/v, 50/50). 4'-Amino-benzo-15-crown-5 (AB15C5) is synthesized from 4'-nitro-benzo-15-crown-5 (Sigma-Aldrich) according to

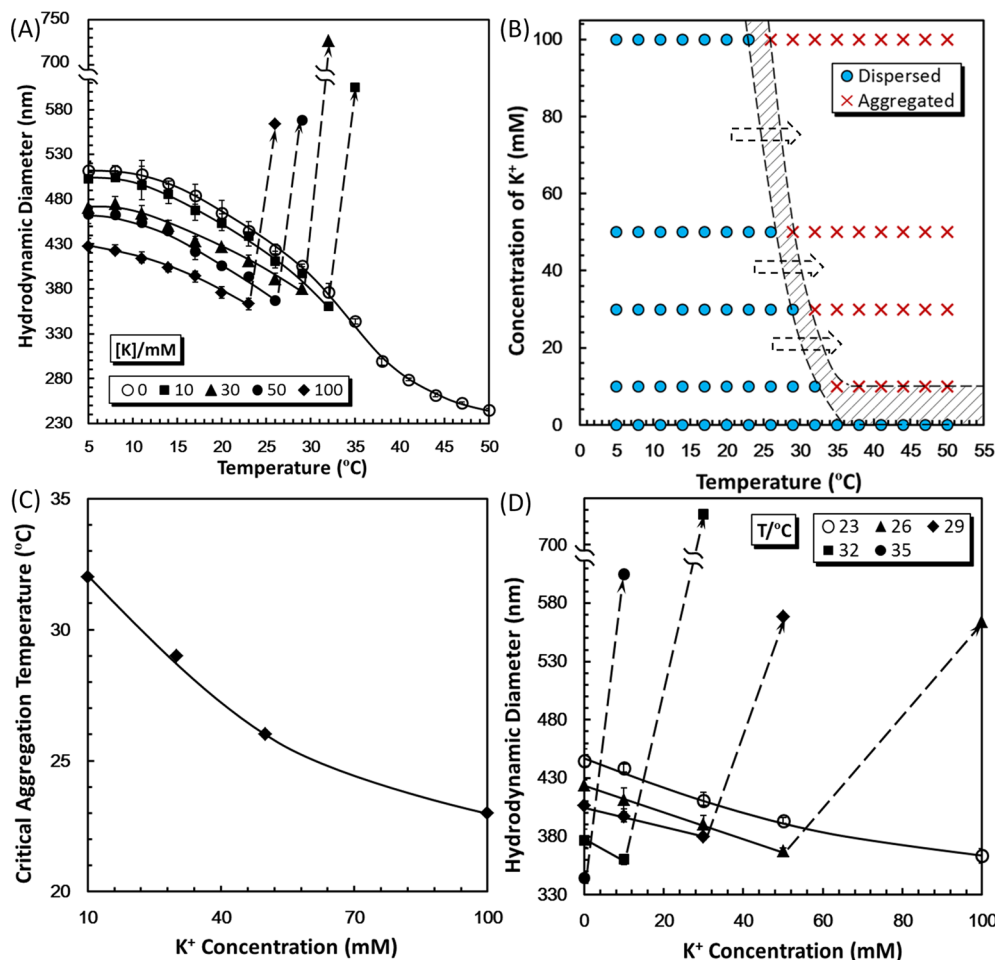


**Figure 5.** K<sup>+</sup>-induced shrinking and aggregating behaviors of P(NIPAM-co-AAB15C5) microspheres prepared with 0.2 mol L<sup>-1</sup> monomer concentration. (A) Hydrodynamic diameters of microspheres as a function of K<sup>+</sup> concentration and temperature. (B) State diagram of the dispersed-to-aggregated transformation of microspheres as a function of K<sup>+</sup> concentration and temperature. (C) Relationship between the K<sup>+</sup> concentration and the critical aggregation temperature. (D) Relationship between the K<sup>+</sup> concentration and the hydrodynamic diameter of the microspheres under a certain temperature condition.

previously reported procedures.<sup>23,24</sup> *N,N'*-Methylenebis-acrylamide (MBA), ammonium persulfate (APS), sodium dodecyl sulfate (SDS), and acrylic acid (AAc) are all purchased from Chengdu Kelong Chemical Reagents. 1-(3-(Dimethylamino)propyl)-3-ethyl carbodiimide hydrochloride (EDC) is purchased from Sigma-Aldrich. All solvents and other chemicals are of analytical grade and used as received. Deionized water (18.2 MΩ, 25 °C) from a Milli-Q Plus water purification system (Millipore) is used throughout this work.

**Preparation of Microspheres.** The proposed P(NIPAM-co-AAB15C5) microspheres are prepared by a two-step reaction method combining precipitation copolymerization<sup>20</sup> and chemical modification.<sup>26</sup> First, poly(*N*-isopropylacrylamide-co-acrylic acid) (P(NIPAM-co-AAc)) microspheres with different compositions (Table 1) are prepared in a single step by thermally initiated free-radical precipitation copolymerization of NIPAM and AAc comonomers with MBA as cross-linker and APS as initiator. The molar ratios of APS and SDS to the total comonomers are kept constant as 1 and 0.8 mol %, respectively. The reaction solution is bubbled with N<sub>2</sub> gas for 20 min to remove dissolved oxygen and then is heated to 70 °C to initiate the copolymerization. The precipitation copolymerization is carried out at 70 °C for 4 h under a N<sub>2</sub> atmosphere. The prepared P(NIPAM-co-AAc) microspheres are purified for 7 days by dialysis (cutoff 8000–15 000 Da) against deionized water, which is refreshed every 12 h. Next, the P(NIPAM-co-AAc) microspheres are modified with AAB15C5 by using EDC as a dehydration catalyst. During the modification process, the dispersion of P(NIPAM-co-AAc) microspheres in deionized water that mixed with AAB15C5 and EDC is stirred below

4 °C for 24 h under the N<sub>2</sub> atmosphere. Then, the obtained P(NIPAM-co-AAB15C5) microspheres are purified by dialysis (cutoff 8000–15 000 Da) against water.

**Compositional and Morphological Characterizations of Microspheres.** The chemical compositions of P(NIPAM-co-AAc) and P(NIPAM-co-AAB15C5) microspheres are confirmed by Fourier transform infrared spectroscopy (FT-IR, IR Prestige-21, Shimadzu) by using the KBr disc technique. The size and morphology of microspheres in the absence and presence of K<sup>+</sup> ions in the dried state are observed by a scanning electron microscope (SEM, JSM-7500F, JEOL). All specimens for SEM measurements are dried at room temperature and sputter-coated with gold before observation.

**Characterization of K<sup>+</sup>-Induced Shrinking and Aggregating Behaviors of Microspheres.** The K<sup>+</sup>-induced shrinking and aggregating behaviors of microspheres are studied by evaluating their size change behaviors in different cation solutions at fixed ambient temperatures ranging from 5 to 50 °C. The hydrodynamic diameters of P(NIPAM-co-AAB15C5) microspheres are measured by dynamic light scattering (DLS, Zetasizer Nano-ZEN3690, Malvern) with highly diluted microsphere dispersions in different aqueous solutions. To minimize salting-out effects, nitrates are chosen as the model salts.<sup>27–29</sup> In consideration of the strong oxidation of HNO<sub>3</sub>, HCl is used to study the effect of H<sup>+</sup>. The data of hydrodynamic diameters of microspheres presented in this paper are the average values of at least three measurements.

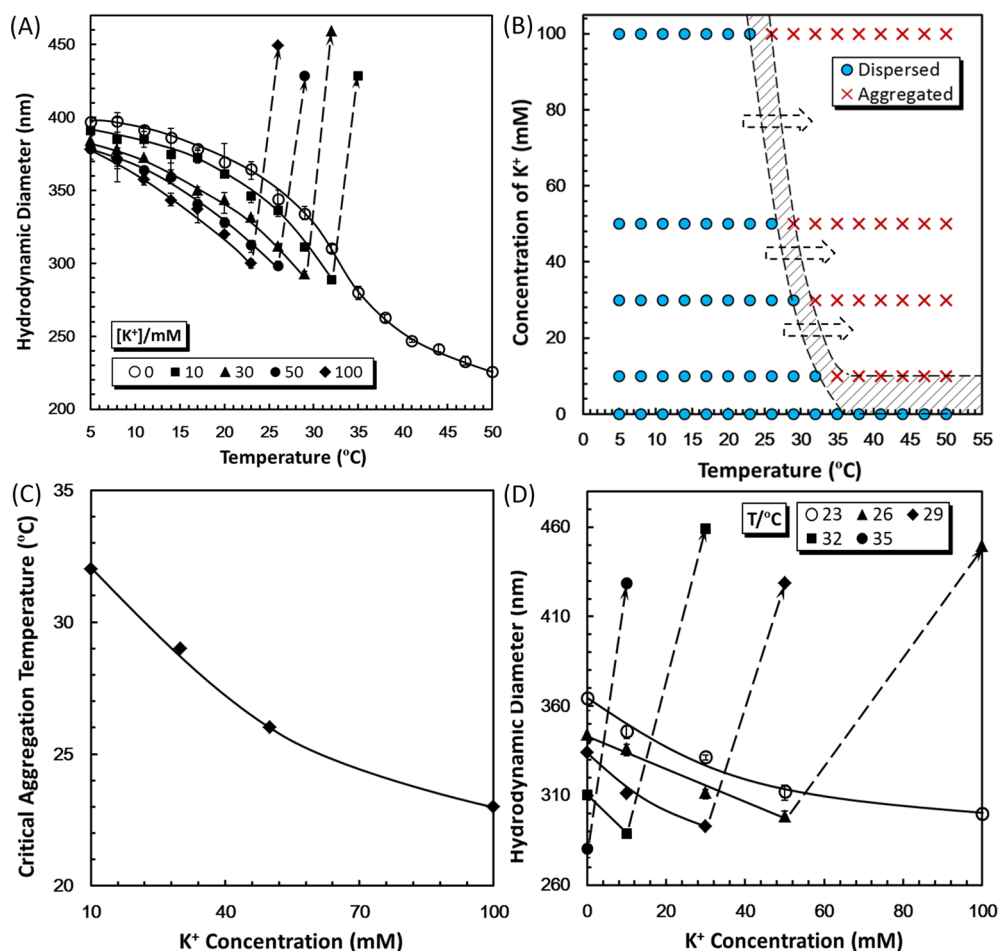


**Figure 6.** K<sup>+</sup>-induced shrinking and aggregating behaviors of P(NIPAM-co-AAB15C5) microspheres prepared with 0.3 mol L<sup>-1</sup> monomer concentration. (A) Hydrodynamic diameters of microspheres as a function of K<sup>+</sup> concentration and temperature. (B) State diagram of the dispersed-to-aggregated transformation of microspheres as a function of K<sup>+</sup> concentration and temperature. (C) Relationship between the K<sup>+</sup> concentration and the critical aggregation temperature. (D) Relationship between the K<sup>+</sup> concentration and the hydrodynamic diameter of the microspheres under a certain temperature condition.

## RESULTS AND DISCUSSION

**Composition and Morphology of Microspheres.** FT-IR spectra of P(NIPAM-co-AAc) and P(NIPAM-co-AAB15C5) microspheres are shown in Figure 2. From the FT-IR spectra, successful fabrications of P(NIPAM-co-AAc) and P(NIPAM-co-AAB15C5) microspheres are confirmed. Specifically, the characteristic bands of the benzo-15-crown-5 group, including a strong peak at 1516 cm<sup>-1</sup> (shoulder peak) for C=C skeletal stretching vibration in the phenyl ring, a peak at 1229 cm<sup>-1</sup> for C–O asymmetric stretching vibration in Ar–O–R, and a peak at 1132 cm<sup>-1</sup> for C–O asymmetric stretching vibration in R–O–R', and double peaks at 1387 and 1368 cm<sup>-1</sup> for the isopropyl group of NIPAM are both found in the FT-IR spectra of P(NIPAM-co-AAB15C5) microspheres prepared with 10% (Curve B), 20% (Curve C), and 30% (Curve D) of AAc feed molar contents. Furthermore, the characteristic peak at 1713 cm<sup>-1</sup> for the carboxylic group of AAc in the FT-IR spectrum of the P(NIPAM-co-AAc) microspheres (Curve A) disappears in the FT-IR spectrum of P(NIPAM-co-AAB15C5) microspheres (Curve B), which indicates that almost all AAc units are converted to AAB15C5 units after the chemical modification. Particularly, the intensity of the characteristic peak of benzo-15-crown-5 group at 1516 cm<sup>-1</sup> for P(NIPAM-co-AAB15C5) microspheres increases with an increase in the AAc feed molar

content, which indicates that a larger amount of AAc feed molar contents leads to a larger amount of crown ether units in the as-prepared P(NIPAM-co-AAB15C5) microspheres.

SEM images of P(NIPAM-co-AAB15C5) microspheres in the absence and presence of 100 mM K<sup>+</sup> ions in the dried state are shown in Figure 3. In the absence of K<sup>+</sup> ions, P(NIPAM-co-AAB15C5) microspheres disperse well and exhibit good spherical shapes and good monodispersity (Figure 3A). The average diameters of dried microspheres in the absence of K<sup>+</sup> ions are about 250 nm. However, in the presence of K<sup>+</sup> ions, microspheres seriously aggregate and their diameters all reduce to about 140 nm due to the formation of 2:1 “sandwich-type” host–guest complexes between 15-crown-5 units and K<sup>+</sup> ions within and among microspheres (Figure 3B).

**Effects of Ion Species and K<sup>+</sup> Concentration on the Isothermal Shrinking and Aggregating Behaviors of Microspheres.** Besides K<sup>+</sup>, five kinds of other common cations, Na<sup>+</sup>, Ca<sup>2+</sup>, Mg<sup>2+</sup>, H<sup>+</sup>, and NH<sub>4</sub><sup>+</sup> are introduced as references to test the isothermal shrinking and aggregating behaviors of microspheres for a comparison. The results show that the P(NIPAM-co-AAB15C5) microspheres are featured with specifically K<sup>+</sup>-recognizable responsive properties. Only K<sup>+</sup> ions can trigger the isothermal shrinking of microspheres due to the formation of stable 2:1 (ligand/ion) “sandwich-type”

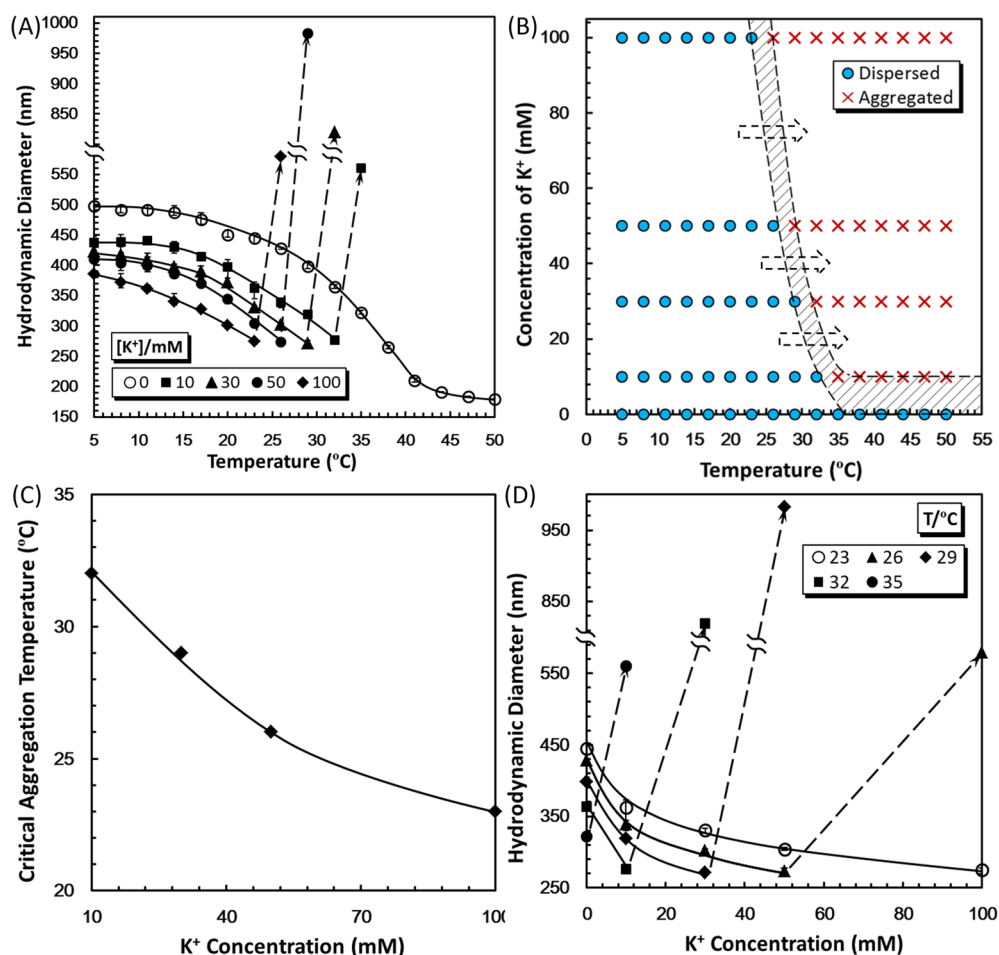


**Figure 7.** K<sup>+</sup>-induced shrinking and aggregating behaviors of P(NIPAM-co-AAB15C5) microspheres prepared with cross-linking degree as 1%. (A) Hydrodynamic diameters of microspheres as a function of K<sup>+</sup> concentration and temperature. (B) State diagram of the dispersed-to-aggregated transformation of microspheres as a function of K<sup>+</sup> concentration and temperature. (C) Relationship between the K<sup>+</sup> concentration and the critical aggregation temperature. (D) Relationship between the K<sup>+</sup> concentration and the hydrodynamic diameter of the microspheres under a certain temperature condition.

host–guest complexes between 15-crown-5 units and K<sup>+</sup> ions. Since other ions cannot form stable 2:1 host–guest complexes with 15-crown-5 units, they cannot trigger the isothermal shrinking of microspheres. As shown in Figure 4A, P(NIPAM-co-AAB15C5) microspheres undergo a rapid volume decrease in deionized water when the ambient temperature increases across a region due to the thermoresponsive property of PNIPAM units. In these cation solutions, the concentrations of the cations are all 0.1 M, and with an increase in the temperature, the hydrodynamic diameters of the microspheres decrease first and then increase dramatically at a certain temperature. It has been reported that dispersions of PNIPAM microspheres exhibit aggregation phenomena in the presence of electrolytes.<sup>30–36</sup> Electrolytes can compete with PNIPAM chains for water molecules, resulting in the dehydration of the PNIPAM chains. Such a dehydration effect decreases the hydrophilicity of P(NIPAM-co-AAB15C5) microspheres and leads to the aggregation of microspheres, which is reflected in the sudden increase of the microsphere diameters in Figure 4A. Figure 4B illustrates the corresponding state diagram of the dispersed-to-aggregated transformation of P(NIPAM-co-AAB15C5) microspheres in deionized water and various cation solutions as a function of temperature. The state diagram shows that the state of P(NIPAM-co-AAB15C5) microspheres is

related to the temperature and the kind of cations. P(NIPAM-co-AAB15C5) microspheres always stay dispersed in deionized water with the temperature ranging from 5 to 50 °C, while in cation solutions, P(NIPAM-co-AAB15C5) microspheres transfer from a dispersed state to an aggregated state at a certain temperature, which is defined as the critical aggregation temperature.<sup>35</sup> Obviously, the critical aggregation temperature of P(NIPAM-co-AAB15C5) microspheres in 0.1 M K<sup>+</sup> solution is much lower than that in other cation solutions, including Na<sup>+</sup>, Ca<sup>2+</sup>, Mg<sup>2+</sup>, H<sup>+</sup>, and NH<sub>4</sub><sup>+</sup> solutions. With K<sup>+</sup> ions as the guests, the isothermal aggregation of P(NIPAM-co-AAB15C5) microspheres can be achieved even at room temperature, e.g., 20 or 25 °C, which is much lower than the lower critical solution temperature (LCST) of PNIPAM; however, in other cation solutions, the isothermal aggregation of microspheres can only be achieved at temperatures very close to the LCST. Such a distinct low critical aggregation temperature of P(NIPAM-co-AAB15C5) microspheres in K<sup>+</sup> solution is resulted from the formation of stable 2:1 “sandwich-type” host–guest complexes of 15-crown-5 and K<sup>+</sup>.<sup>21,22</sup> Such a complexation action can disrupt the hydrogen bonding between oxygen atoms in crown ether and hydrogen atoms of water, which results in the aggregation phenomenon of microspheres in K<sup>+</sup> solution at low temperatures.

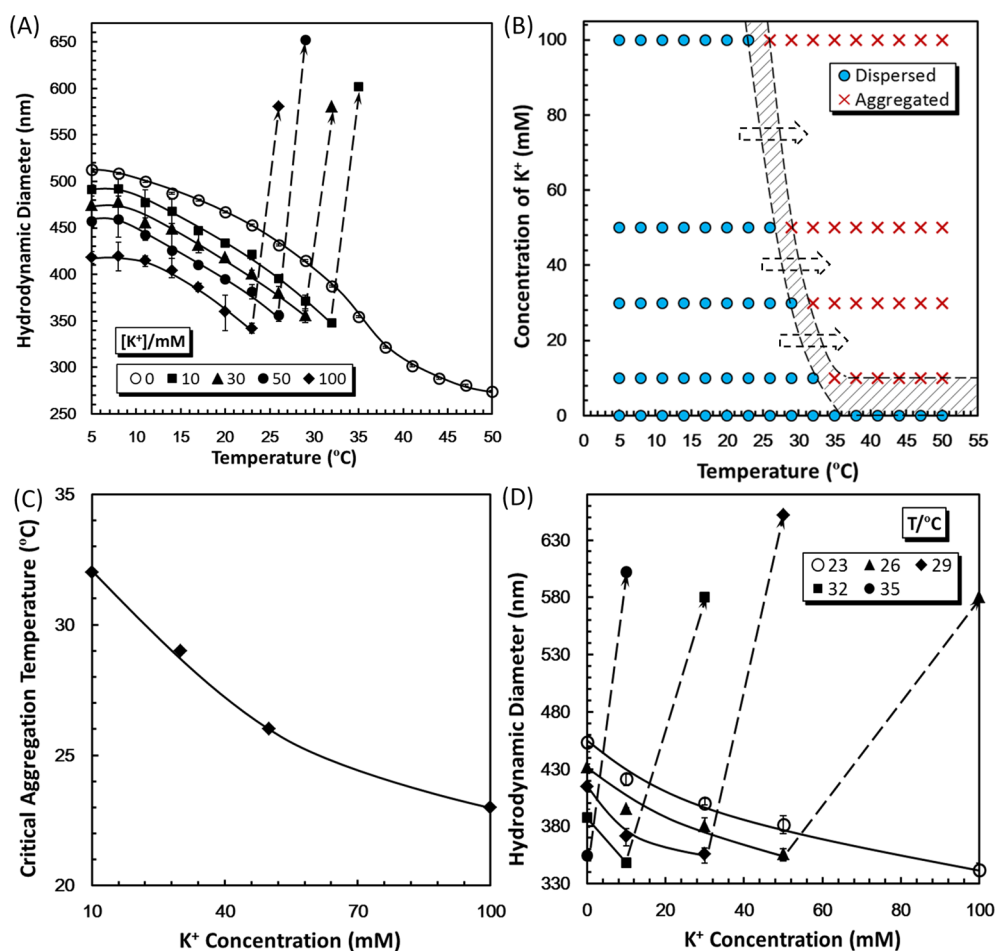


**Figure 8.** K<sup>+</sup>-induced shrinking and aggregating behaviors of P(NIPAM-co-AAB15C5) microspheres prepared with cross-linking degree as 5%. (A) Hydrodynamic diameters of microspheres as a function of K<sup>+</sup> concentration and temperature. (B) State diagram of the dispersed-to-aggregated transformation of microspheres as a function of K<sup>+</sup> concentration and temperature. (C) Relationship between the K<sup>+</sup> concentration and the critical aggregation temperature. (D) Relationship between the K<sup>+</sup> concentration and the hydrodynamic diameter of the microspheres under a certain temperature condition.

Effects of environmental K<sup>+</sup> concentration and temperature on the K<sup>+</sup>-induced shrinking and aggregating behaviors of microspheres are shown in Figure 4C–F. In this study, the range of K<sup>+</sup> concentrations is from 0 to 100 mM. In the state diagram (Figure 4D), the dispersed-state region is located in the lower left region and the aggregated-state region is located in the upper right region. These two regions are separated by a narrow region of critical aggregation temperature and critical aggregation K<sup>+</sup> concentration. Microspheres are more likely to get aggregated when the surrounding K<sup>+</sup> concentration is high. There is an inverse relationship between the critical aggregation temperature and the critical aggregation K<sup>+</sup> concentration. The critical aggregation temperature decreases with an increase in the K<sup>+</sup> concentration (Figure 4E), and the critical aggregation temperature can be as low as 20 °C when the K<sup>+</sup> concentration is 100 mM, while the critical aggregation K<sup>+</sup> concentration decreases with an increase in the environmental temperature (Figure 4F). When the environmental temperature is 32 °C, microspheres can aggregate at a low K<sup>+</sup> concentration, which is lower than 10 mM. That is, the dispersed/aggregated state of P(NIPAM-co-AAB15C5) microspheres can be tuned by varying the temperature and K<sup>+</sup> concentration. Such a tunable K<sup>+</sup>-induced aggregating property of P(NIPAM-co-AAB15C5)

microsphere provides a novel model for designing targeted drug delivery systems.

Up to now, most reported works related to PNIPAM-based microspheres with metal ion-induced aggregating property are in response to Na<sup>+</sup> ions, which are mainly the flocculation behaviors of PNIPAM-based microspheres caused by sodium salts and temperature.<sup>31–34,36</sup> Only a few works are related to PNIPAM microspheres with K<sup>+</sup>-induced aggregating property. It has been reported that PNIPAM microgels exhibit K<sup>+</sup>-induced aggregating property because of the salting-out effect at a very high K<sup>+</sup> concentration, which is larger than 100 mM.<sup>35</sup> However, the K<sup>+</sup>-induced aggregating property only at a high K<sup>+</sup> concentration restricts its use in biomedical applications. The P(NIPAM-co-B18C6Am) microspheres are reported to exhibit K<sup>+</sup>-induced swelling and aggregating property due to the formation of stable 1:1 “host-guest” 18-crown-6/K<sup>+</sup> complexes.<sup>20</sup> Unfortunately, K<sup>+</sup>-induced swelling behavior may be unsuitable for certain applications, such as K<sup>+</sup>-triggered release of drugs. Thus, compared with the previously reported works, the microspheres proposed in this study with synchronously K<sup>+</sup>-induced shrinking and aggregating property at a low K<sup>+</sup> concentration exhibit novelty, and the results provide valuable guidance for designing novel targeted drug delivery systems.

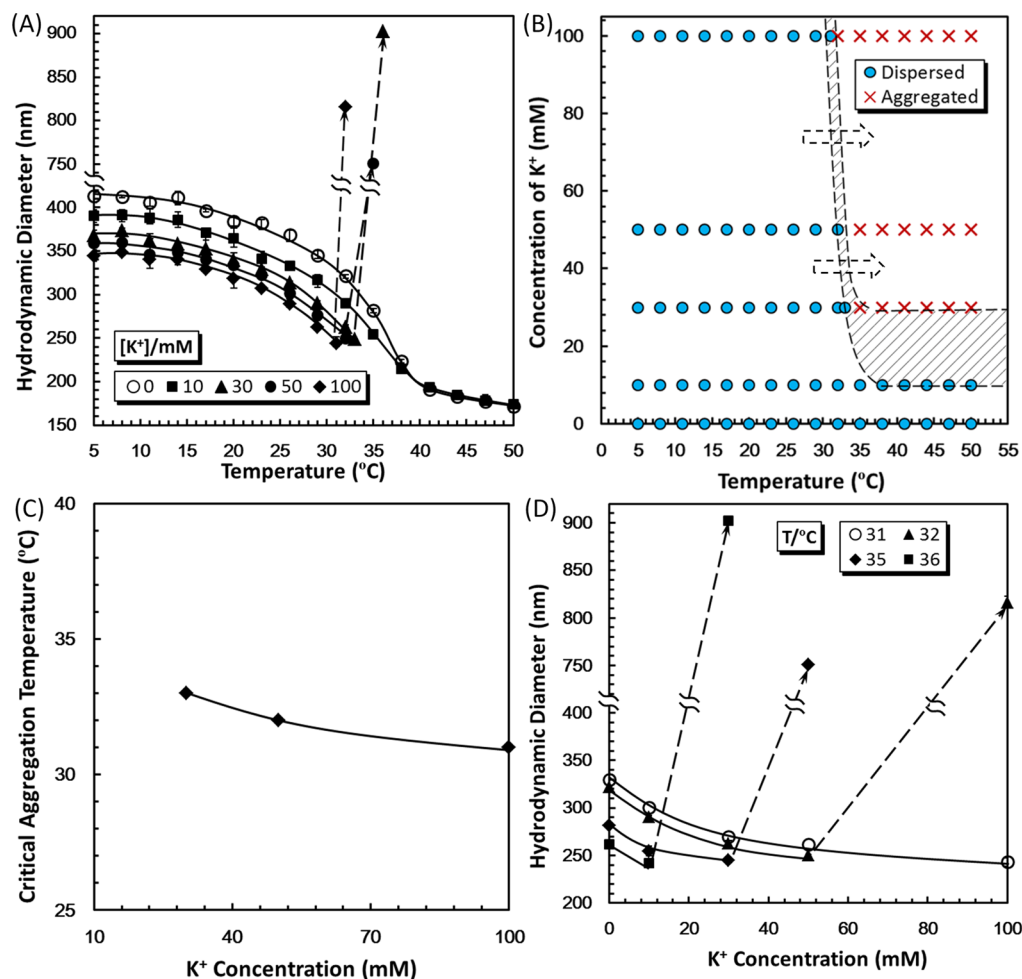


**Figure 9.** K<sup>+</sup>-induced shrinking and aggregating behaviors of P(NIPAM-co-AAB15C5) microspheres prepared with 10% AAc feed molar content ([AAc]/[NIPAM + AAc]). (A) Hydrodynamic diameters of microspheres as a function of K<sup>+</sup> concentration and temperature. (B) State diagram of the dispersed-to-aggregated transformation of microspheres as a function of K<sup>+</sup> concentration and temperature. (C) Relationship between the K<sup>+</sup> concentration and the critical aggregation temperature. (D) Relationship between the K<sup>+</sup> concentration and the hydrodynamic diameter of the microspheres under a certain temperature condition.

### Effects of Chemical Compositions of Microspheres on the K<sup>+</sup>-Induced Shrinking and Aggregating Properties.

K<sup>+</sup>-induced shrinking and aggregating behaviors of P(NIPAM-co-AAB15C5) microspheres prepared with different monomer concentrations are shown in Figures 5 and 6. The concentration of total monomers ([NIPAM] + [AAc]) is varied as 0.2 and 0.3 mol L<sup>-1</sup> while keeping the other parameters constant. P(NIPAM-co-AAB15C5) microspheres all exhibit good K<sup>+</sup>-induced shrinking and aggregating behaviors in K<sup>+</sup> solutions with various concentrations. Although the K<sup>+</sup>-induced shrinking behaviors of P(NIPAM-co-AAB15C5) microspheres prepared with these two monomer concentrations are different (Figures 5A and 6A; Figures 5D and 6D), the K<sup>+</sup>-induced aggregating behaviors of these two batch of microspheres are almost the same (Figures 5B and 6B; Figures 5C and 6C). That is, the variation of monomer concentration nearly does not affect the K<sup>+</sup>-induced aggregation properties of P(NIPAM-co-AAB15C5) microspheres. The K<sup>+</sup>-induced aggregation sensitivity is related to the amount of the formed “sandwich-type” host–guest complexes between crown ethers and K<sup>+</sup> ions. The amount of crown ether units in the as-prepared microspheres is not influenced by the variation of monomer concentration; therefore, the K<sup>+</sup>-induced aggregation sensitivity

of microspheres cannot be regulated by varying the monomer concentration in microsphere preparation.

K<sup>+</sup>-induced shrinking and aggregating behaviors of P(NIPAM-co-AAB15C5) microspheres prepared with different cross-linking degrees are shown in Figures 7 and 8. Just as the above-mentioned case of monomer concentration, although the K<sup>+</sup>-induced shrinking behaviors of P(NIPAM-co-AAB15C5) microspheres prepared with cross-linking degrees of 1% and 5% are different (Figures 7A and 8A; Figures 7D and 8D), the K<sup>+</sup>-induced aggregating behaviors of these microspheres are almost the same (Figures 7B and 8B; Figures 7C and 8C). That is, the K<sup>+</sup>-induced aggregation sensitivity of microspheres cannot be regulated by varying the cross-linking degree of the microspheres either.

K<sup>+</sup>-induced shrinking and aggregating behaviors of P(NIPAM-co-AAB15C5) microspheres prepared with different AAc feed molar contents ([AAc]/[NIPAM + AAc]) are shown in Figures 9 and 10. Obviously, the K<sup>+</sup>-induced shrinking and aggregating behaviors of P(NIPAM-co-AAB15C5) microspheres prepared with 10% and 30% [AAc]/[NIPAM + AAc] are both significantly different. For the microspheres prepared with 10% [AAc]/[NIPAM + AAc] (Figure 9), K<sup>+</sup> with a concentration of 10 mM cannot even trigger the aggregation, and



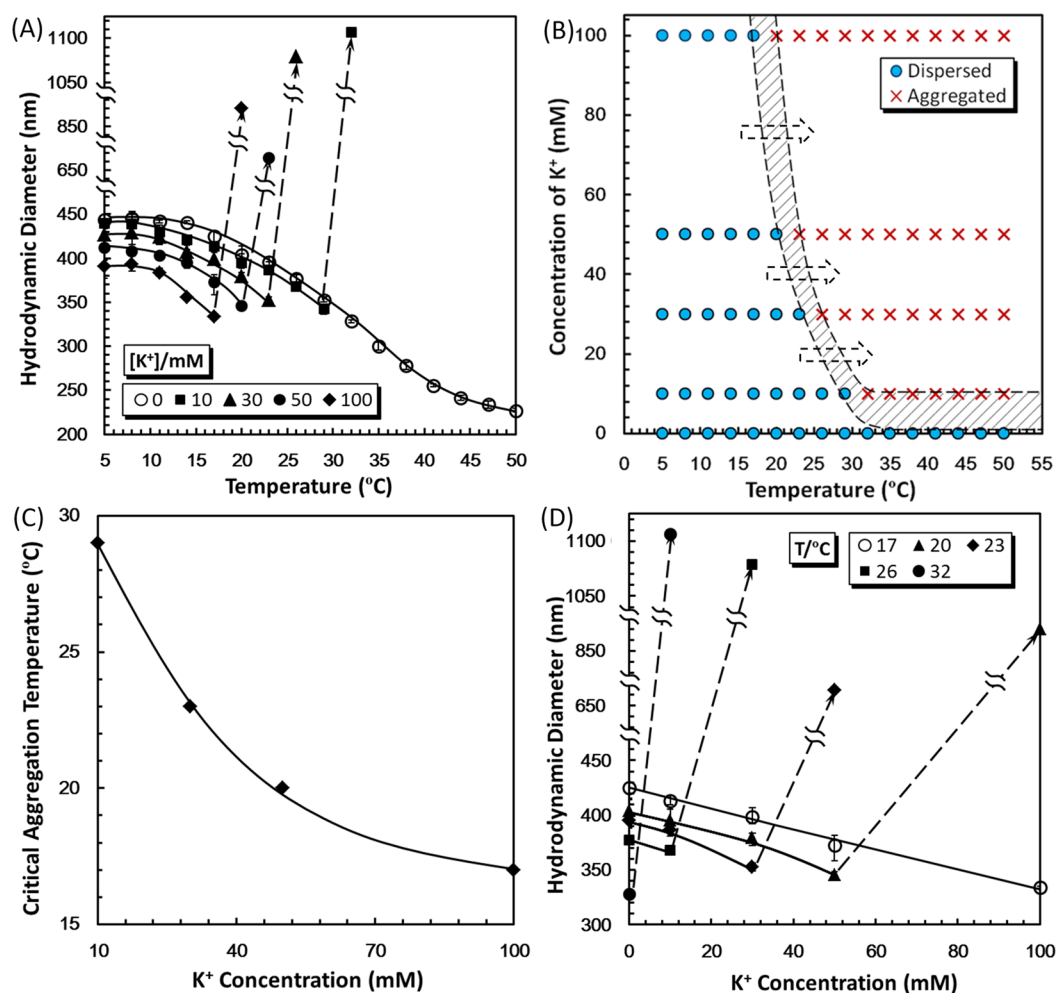


**Figure 10.** K<sup>+</sup>-induced shrinking and aggregating behaviors of P(NIPAM-co-AAB15C5) microspheres prepared with 30% AAc feed molar content ([AAc]/[NIPAM + AAc]). (A) Hydrodynamic diameters of microspheres as a function of K<sup>+</sup> concentration and temperature. (B) State diagram of the dispersed-to-aggregated transformation of microspheres as a function of K<sup>+</sup> concentration and temperature. (C) Relationship between the K<sup>+</sup> concentration and the critical aggregation temperature. (D) Relationship between the K<sup>+</sup> concentration and the hydrodynamic diameter of the microspheres under a certain temperature condition.

the critical aggregation K<sup>+</sup> concentration is located between 10 and 30 mM no matter how the environmental temperature changes. However, for the microspheres prepared with 30% [AAc]/[NIPAM + AAc] (Figure 10), the critical aggregation K<sup>+</sup> concentration is much lower, which is below 10 mM. When the K<sup>+</sup> concentration is the same, the critical aggregation temperature of microspheres prepared with a larger AAc feed molar content is much lower than that of microspheres prepared with a smaller AAc feed molar content. The aggregated-state area located in the upper right region of the P(NIPAM-co-AAB15C5) microspheres prepared with a larger AAc feed molar content is much larger than that of microspheres prepared with a smaller AAc feed molar content, which indicates that P(NIPAM-co-AAB15C5) microspheres prepared with a larger AAc feed molar content exhibit higher K<sup>+</sup>-induced aggregating sensitivity. As has been confirmed by the FT-IR characterization in Figure 2, the higher the AAc feed molar content, the larger is the amount of crown ether units in the as-prepared P(NIPAM-co-AAB15C5) microspheres. As a result, more 2:1 “sandwich-type” host–guest complexes between 15-crown-5 units and K<sup>+</sup> ions can form within and among the microspheres prepared with the higher AAc feed

molar content; thus, the K<sup>+</sup>-induced aggregation of microspheres is more sensitive.

## CONCLUSIONS

A novel type of smart microspheres with K<sup>+</sup>-induced shrinking and aggregating properties based on a responsive host–guest system has been successfully developed for the first time. The microspheres are composed of cross-linked P(NIPAM-co-AAB15C5) networks and prepared by a two-step reaction method combining precipitation copolymerization and chemical modification. The prepared microspheres exhibit significant K<sup>+</sup>-induced shrinking and aggregating properties, due to the formation of stable 2:1 “sandwich-type” host–guest complexes between 15-crown-5 units on the P(NIPAM-co-AAB15C5) networks and K<sup>+</sup> ions, while other cations (e.g., Na<sup>+</sup>, H<sup>+</sup>, NH<sub>4</sub><sup>+</sup>, Mg<sup>2+</sup>, or Ca<sup>2+</sup>) cannot trigger such response behaviors. The K<sup>+</sup>-induced aggregation of microspheres can be achieved effectively under the condition of low K<sup>+</sup> concentration, because enough 15-crown-5 units can be introduced onto the polymeric networks of the microspheres by the proposed two-step reaction method in this study. The K<sup>+</sup>-induced aggregating sensitivity of the P(NIPAM-co-AAB15C5) microspheres can be enhanced by increasing the content of crown ether units in the

polymeric networks; however, it is nearly not influenced by varying the monomer and cross-linker concentrations in the microsphere preparation. According to the experimental data, state diagrams of the dispersed-to-aggregated transformation of P(NIPAM-co-AAB15C5) microspheres as a function of environmental temperature and  $K^+$  concentration have been constructed. The dispersed/aggregated state of the microspheres can be tuned by varying environmental temperature and  $K^+$  concentration. The results in this study provide valuable guidance for designing and developing novel functional microspheres with  $K^+$ -recognizable shrinking and aggregating properties for biomedical applications.

## AUTHOR INFORMATION

### Corresponding Authors

\*E-mail: chuly@scu.edu.cn.

\*E-mail: juxiaojie@scu.edu.cn.

### Notes

The authors declare no competing financial interest.

## ACKNOWLEDGMENTS

The authors gratefully acknowledge support from the National Natural Science Foundation of China (21322605, 81321002) and the Program for Changjiang Scholars and Innovative Research Team in University (IRT1163).

## REFERENCES

- Berg, J. M.; Tymoczko, J. L.; Stryer, L. *Biochemistry*, 5th ed; W. H. Freeman and Company: New York, 2002.
- Kuo, H. C.; Cheng, C. F.; Clark, R. B.; Lin, J. J.-C.; Lin, J. L.-C.; Hoshijima, M.; Nguyễn-Trần, V. T. B.; Gu, Y.; Ikeda, Y.; Chu, P.-H.; Ross, J.; Giles, W. R.; Chien, K. R. A Defect in the  $K^+$  Channel-Interacting Protein 2 (KChIP2) Gene Leads to a Complete Loss of  $I_{to}$  and Confers Susceptibility to Ventricular Tachycardia. *Cell* **2001**, *107*, 801–813.
- Clausen, T.  $Na^+K^+$  Pump Regulation and Skeletal Muscle Contractility. *Physiol. Rev.* **2003**, *83*, 1269–1324.
- Gao, Y. F.; Serpe, M. J. Light-Induced Color Changes of Microgel-Based Etalons. *ACS Appl. Mater. Interfaces* **2014**, *6*, 8461–8466.
- Soppimath, K. S.; Tan, D. C.-W.; Yang, Y. Y. pH-Triggered Thermally Responsive Core-Shell Nanoparticles for Drug Delivery. *Adv. Mater.* **2005**, *17*, 318–323.
- Karg, M.; Isabel, P. S.; Benito, R. G.; Klitzing, R. V.; Wellert, S.; Hellweg, T. Temperature, pH, and Ionic Strength Induced Changes of the Swelling Behavior of PNIPAM-Poly(allylacetic acid) Copolymer Microgels. *Langmuir* **2008**, *24*, 6300–6306.
- Chen, H.; Dai, L. L. Adsorption and Release of Active Species into and from Multifunctional Ionic Microgel Particles. *Langmuir* **2013**, *29*, 11227–11235.
- Xing, S. Y.; Guan, Y.; Zhang, Y. J. Kinetics of Glucose-Induced Swelling of P(NIPAM-AAPBA) Microgels. *Macromolecules* **2011**, *44*, 4479–4486.
- Suedee, R.; Jantarat, C.; Lindner, W.; Viernstein, H.; Songkro, S.; Srichana, T. Development of a pH-Responsive Drug Delivery System for Enantioselective-Controlled Delivery of Racemic Drugs. *J. Controlled Release* **2010**, *142*, 122–131.
- Sivakumaran, D.; Maitland, D.; Hoare, T. Injectable Microgel-Hydrogel Composites for Prolonged Small-Molecule Drug Delivery. *Biomacromolecules* **2011**, *12*, 4112–4120.
- Ghugare, S. V.; Mozetic, P.; Paradossi, G. Temperature-Sensitive Poly(vinyl alcohol)/Poly(methacrylate-co-N-isopropyl acrylamide) Microgels for Doxorubicin Delivery. *Biomacromolecules* **2009**, *10*, 1589–1596.
- Chang, B. S.; Sha, X. Y.; Guo, J.; Jiao, Y. F.; Wang, C. C.; Yang, W. L. Thermo and pH Dual Responsive, Polymer Shell Coated, Magnetic Mesoporous Silica Nanoparticles for Controlled Drug Release. *J. Mater. Chem.* **2011**, *21*, 9239–9247.
- Islam, M. R.; Serpe, M. J. Polyelectrolyte Mediated Intra and Intermolecular Crosslinking in Microgel-Based Etalons for Sensing Protein Concentration in Solution. *Chem. Commun.* **2013**, *49*, 2646–2648.
- Zhou, Y. Y.; Tang, L.; Zeng, G. M.; Chen, J.; Cai, Y.; Zhang, Y.; Yang, G. D.; Liu, Y. Y.; Zhang, C.; Tang, W. W. Mesoporous Carbon Nitride Based Biosensor for Highly Sensitive and Selective Analysis of Phenol and Catechol in Compost Bioremediation. *Biosens. Bioelectron.* **2014**, *61*, 519–525.
- Tang, L.; Yang, G. D.; Zeng, G. M.; Cai, Y.; Li, S. S.; Zhou, Y. Y.; Pang, Y.; Liu, Y. Y.; Zhang, Y.; Luna, B. Synergistic Effect of Iron Doped Ordered Mesoporous Carbon on Adsorption-Coupled Reduction of Hexavalent Chromium and the Relative Mechanism Study. *Chem. Eng. J.* **2014**, *239*, 114–122.
- Häfele, U. O.; Saatchi, K.; Elischer, P.; Misri, R.; Bokharaei, M.; Labiris, N. R.; Stoeber, B. Lung Perfusion Imaging with Monosized Biodegradable Microspheres. *Biomacromolecules* **2010**, *11*, 561–567.
- Zhou, M. Y.; Chu, L. Y.; Chen, W. M.; Ju, X. J. Flow and Aggregation Characteristics of Thermo-Responsive Poly(N-isopropylacrylamide) Spheres during the Phase Transition. *Chem. Eng. Sci.* **2006**, *61*, 6337–6347.
- Zhou, M. Y.; Xie, R.; Ju, X. J.; Zhao, Z. L.; Chu, L. Y. Flow Characteristics of Thermo-Responsive Microspheres in Microchannel during the Phase Transition. *AIChE J.* **2009**, *55*, 1559–1568.
- Ito, T.; Hioki, T.; Yamaguchi, T.; Shinbo, T.; Nakao, S.; Kimura, S. Development of a Molecular Recognition Ion Gating Membrane and Estimation of Its Pore Size Control. *J. Am. Chem. Soc.* **2002**, *124*, 7840–7846.
- Ju, X. J.; Liu, L.; Xie, R.; Niu, C. H.; Chu, L. Y. Dual Thermo-Responsive and Ion-Recognizable Monodisperse Microspheres. *Polymer* **2009**, *50*, 922–929.
- Yamauchi, A.; Hayashita, T.; Nishizawa, S.; Watanabe, M.; Teramae, N. Benzo-15-crown-5 Fluoroionophore/ $\gamma$ -Cyclodextrin Complex with Remarkably High Potassium Ion Sensitivity and Selectivity in Water. *J. Am. Chem. Soc.* **1999**, *121*, 2319–2320.
- Xia, W. S.; Schmehl, R. H.; Li, C. J. A Highly Selective Fluorescent Chemosensor for  $K^+$  from a Bis-15-crown-5 Derivative. *J. Am. Chem. Soc.* **1999**, *121*, 5599–5600.
- Mi, P.; Chu, L. Y.; Ju, X. J.; Niu, C. H. A Smart Polymer with Ion-Induced Negative Shift of the Lower Critical Solution Temperature for Phase Transition. *Macromol. Rapid Commun.* **2008**, *29*, 27–32.
- Mi, P.; Ju, X. J.; Xie, R.; Wu, H. G.; Ma, J.; Chu, L. Y. A Novel Stimuli-Responsive Hydrogel for  $K^+$ -Induced Controlled-Release. *Polymer* **2010**, *51*, 1648–1653.
- Yu, H. R.; Ju, X. J.; Xie, R.; Wang, W.; Zhang, B.; Chu, L. Y. Portable Diagnosis Method of Hyperkalemia Using Potassium-Recognizable Poly(N-isopropylacrylamide-co-benzo-15-crown-5-acrylamide) Copolymers. *Anal. Chem.* **2013**, *85*, 6477–6484.
- Liu, Z.; Luo, F.; Ju, X. J.; Xie, R.; Luo, T.; Sun, Y. M.; Chu, L. Y. Positively  $K^+$ -Responsive Membranes with Functional Gates Driven by Host-Guest Molecular Recognition. *Adv. Funct. Mater.* **2012**, *22*, 4742–4750.
- Inomata, H.; Goto, S.; Otake, K.; Saito, S. Effect of Additives on Phase Transition of N-isopropylacrylamide Gels. *Langmuir* **1992**, *8*, 687–690.
- Zhang, Y. J.; Furryk, S.; Bergbreiter, D. E.; Cremer, P. S. Specific Ion Effects on the Water Solubility of Macromolecules: PNIPAM and the Hofmeister Series. *J. Am. Chem. Soc.* **2005**, *127*, 14505–14510.
- Zhang, Y.; Furryk, S.; Sagle, L. B.; Cho, Y.; Bergbreiter, D. E.; Cremer, P. S. Effects of Hofmeister Anions on the LCST of PNIPAM as a Function of Molecular Weight. *J. Phys. Chem. C* **2007**, *111*, 8916–8924.
- López-León, T.; Ortega-Vinuesa, J. L.; Bastos-González, D.; Elaissari, A. Cationic and Anionic Poly(N-isopropylacrylamide) Based Submicron Gel Particles: Electrokinetic Properties and Colloidal Stability. *J. Phys. Chem. B* **2006**, *110*, 4629–4636.

(31) Daly, E.; Saunders, B. R. Temperature-Dependent Electrophoretic Mobility and Hydrodynamic Radius Measurements of Poly(*N*-isopropylacrylamide) Microgel Particles: Structural Insights. *Phys. Chem. Chem. Phys.* **2000**, *2*, 3187–3193.

(32) Rasmusson, M.; Vincent, B. Flocculation of Microgel Particles. *React. Funct. Polym.* **2004**, *58*, 203–211.

(33) Fanaian, S.; Al-Manasir, N.; Zhu, K. Z.; Kjoniksen, A.-L.; Nyström, B. Effects of Hofmeister Anions on the Flocculation Behavior of Temperature-Responsive Poly(*N*-isopropylacrylamide) Microgels. *Colloid Polym. Sci.* **2012**, *290*, 1609–1616.

(34) Rasmusson, M.; Routh, A.; Vincent, B. Flocculation of Microgel Particles with Sodium Chloride and Sodium Polystyrene Sulfonate as a Function of Temperature. *Langmuir* **2004**, *20*, 3536–3542.

(35) Daly, E.; Saunders, B. R. A Study of the Effect of Electrolyte on the Swelling and Stability of Poly(*N*-isopropylacrylamide) Microgel Dispersions. *Langmuir* **2000**, *16*, 5546–5552.

(36) Liao, W.; Zhang, Y. J.; Guan, Y.; Zhu, X. X. Gelation Kinetics of Thermosensitive PNIPAM Microgel Dispersions. *Macromol. Chem. Phys.* **2011**, *212*, 2052–2060.